

Note on Chern number

Ning Sun
(Dated: November 26, 2016)

Contents

I. Chern number discretized	1
II. Chern number in higher dimensions	5
Acknowledgments	7
References	8
A. Time-dependent Rice-Mele model	8

I. CHERN NUMBER DISCRETIZED

Follow the method that Fukui et.al. has developed in [1], we summarize here the simple way to calculate Chern number numerically in discretized parameter space.

a. Several things to be noticed:

- We restrict our discussion within physical systems of periodical lattice (or what like a periodical lattice) which could be well understood under the band theory frame.
- We point out here that this method is essentially a process of construction of Wilson loop at each plaquette of the discretized parameter space (mostly, torus).
- This method avoid of a procedure of smoothing gauge, an advantage based on merit of last point, that is Wilson loop is gauge-independent.

b. 1st Chern class Here we restrict our discussion within 2-dimensional cases, i.e. the 1st Chern number are we to calculate.

Chern number is defined as

$$c_n = \frac{1}{4\pi} \iint d^2\mathbf{k} (\partial_{k_1} \hat{n} \times \partial_{k_2} \hat{n}) \cdot \hat{n} \quad (1)$$

where the direction vector \hat{n} is as a function of 2d parameter \mathbf{k} , i.e. $\hat{n} = \hat{n}(\mathbf{k}) = \hat{n}(k_1, k_2)$. And \hat{n} characterize, for a physical system, the direction of the underlying state varying with parameters (k_1, k_2) . For example, $\hat{n} = h(\mathbf{q})/|h(\mathbf{q})|$ with $h(\mathbf{q})$ the parametrized Hamiltonian in \mathbf{q} -space for a two-level system when we consider the Chern number of the upper band.

For a lattice system with $|n(\mathbf{k})\rangle$ as its periodic Bloch wave-function of n th band, we define Berry connection and

Berry curvature as

$$\begin{aligned}\mathcal{A}_\mu^{(n)} &= i \langle n(\mathbf{k}) | \partial_\mu n(\mathbf{k}) \rangle \\ \mathcal{F}_{\mu\nu}^{(n)} &= \partial_\mu \mathcal{A}_\nu - \partial_\nu \mathcal{A}_\mu \\ &= i \left[\langle \partial_\mu n(\mathbf{k}) | \partial_\nu n(\mathbf{k}) \rangle - \langle \partial_\nu n(\mathbf{k}) | \partial_\mu n(\mathbf{k}) \rangle \right]\end{aligned}$$

Then we introduce the 1st Chern number to characterize the integral of Berry field defined on a torus $k_x \times k_y$ as

$$\begin{aligned}c_n &= \frac{1}{2\pi} \iint d^2\mathbf{k} \mathcal{F}_{xy}^{(n)}(\mathbf{k}) \\ &= \frac{1}{2\pi} \iint d^2\mathbf{k} i \left[\langle \partial_x n(\mathbf{k}) | \partial_y n(\mathbf{k}) \rangle - \langle \partial_y n(\mathbf{k}) | \partial_x n(\mathbf{k}) \rangle \right]\end{aligned}$$

c. Numerical procedures

1. Discretize parameter space. Always, it's a torus, by which we mean there are two independent parameters, denoted as k_x, k_y , varying along $0 < k_x \leq 1, 0 < k_y \leq 1$, and we identify each pair of two sides (left and right, top and bottom). Also could be other boundary values, not necessary $(0, 1]$, as long as we keep each pair of sides identified. Discretizing the parameter torus we get a set of $N \times N$ points each with a coordinate (x_i, y_j) . N is the total number of one dimension of the parameter space divided into plaquette.

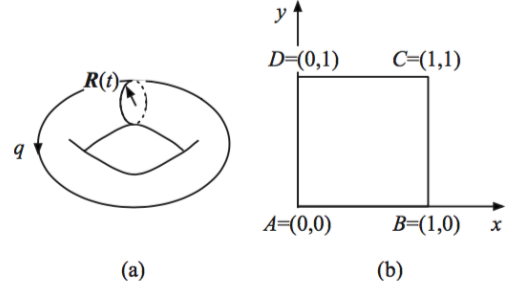


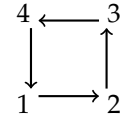
FIG. 1: Schematic torus topology, from [2]

We call it (specifically, this set) the *discretized parameter space*.

2. Diagonalizing Hamiltonian $\mathcal{H}(\mathbf{k})$ at each single points $\mathbf{k} = (x_i, y_j)$ of the discretized parameter space, to obtain a set of eigenvalues $\{\mathcal{E}_n(\mathbf{k})\}$ and corresponding eigenvectors $\{|n(\mathbf{k})\rangle\}$. n is the band index.

Again, we require no gauge smoothing procedure, which means that at each parameter point $\mathbf{k} = (x_i, y_j)$ there has been chosen an arbitrary gauge for the wave function $\{|n(\mathbf{k})\rangle\}$ given by computer program that it could be quite not smooth for two near parameter points \mathbf{k}_1 and \mathbf{k}_2 , i.e. the wave functions at \mathbf{k}_1 and \mathbf{k}_2 might differs a lot. While this results in some singularity in calculating $\mathcal{A}(\mathbf{k})$ using numerically differentiation method, it does not affect the calculation of Berry field $\mathcal{F}(\mathbf{k})$ as well as its integral the Chern number c_n . This attributes to the gauge-independency of Wilson loop, which would be seen in later steps.

3. For each parameter point in the discretized parameter space we have obtained in the first step, we construct a Wilson loop around the plaquette locates at this point.



In numerical calculation, the loop of a plaquette at parameter point $\mathbf{k} = (x_i, y_j)$ is chosen as

$$(x_i, y_j) \rightarrow (x_{i+1}, y_j) \rightarrow (x_{i+1}, y_{j+1}) \rightarrow (x_i, y_{j+1}) \rightarrow (x_i, y_j)$$

with

$$i = 1, 2, 3, \dots, N-1$$

$$j = 1, 2, 3, \dots, N-1$$

Note that the choice might be somewhat “unsymmetrical” in calculating the Berry field strength due to discretization of parameter space. But this would not make big difference in calculation of Chern number as long as we discretize it enough and also makes good approximation to the Berry field (curvature) strength at all points of parameter space.

4. Define for each plaquette

$$\begin{aligned} U_{12} &= V^\dagger(\mathbf{k}_2)V(\mathbf{k}_1) \\ U_{23} &= V^\dagger(\mathbf{k}_3)V(\mathbf{k}_2) \\ U_{34} &= V^\dagger(\mathbf{k}_4)V(\mathbf{k}_3) \\ U_{41} &= V^\dagger(\mathbf{k}_1)V(\mathbf{k}_4) \end{aligned}$$

where $V(\mathbf{k})$ is the unitary matrix diagonalizing Hamiltonian at \mathbf{k} , i.e. the row vector of $V(\mathbf{k})$ is normalized eigenvectors of $\mathcal{H}(\mathbf{k})$,

$$V^\dagger(\mathbf{k})\mathcal{H}(\mathbf{k})V(\mathbf{k}) = D(\mathbf{k})$$

Extract diagonal elements of each link operator U_{ij} , that is, define new link quantity as

$$\mathcal{U}_{ij} = \text{diag}(U_{ij})$$

where $\text{diag}()$ means to retain all diagonal elements of a matrix while abandon all off-diagonal elements. Easy to see that \mathcal{U}_{ij} are all diagonal matrices. And $\mathcal{U}_{ij}^{mn} = \delta_{mn}\mathcal{U}_{ij}^{nn}$.

Define at each $\mathbf{k} = (x_i, y_j)$

$$T_{\text{loop}}(\mathbf{k}) = \mathcal{U}_{41}\mathcal{U}_{34}\mathcal{U}_{23}\mathcal{U}_{12}$$

The Chern number for n th band is calculated through

$$c_n = \frac{1}{2\pi} \sum_{i=1}^{N-1} \sum_{j=1}^{N-1} -i \log T_{\text{loop}}^{(nn)}(x_i, y_j) \quad (2)$$

i.e. sum over the angle of the n th diagonal element of $T_{\text{loop}}(\mathbf{k})$ at all $\mathbf{k} = (x_i, y_j)$.

Berry field at each discretized parameter plaquette for the n th band is just

$$\mathcal{F}_{xy}^{(n)}(\mathbf{k}) = \theta_n(\mathbf{k})/s(\mathbf{k})$$

where $\theta_n(\mathbf{k})$ is the angle of the n th diagonal element of $T_{\text{loop}}(\mathbf{k})$ and $s(\mathbf{k})$ is the area for each plaquette.

$$\theta_n(\mathbf{k}) = -i \log T_{\text{loop}}^{(nn)}(x_i, y_j)$$

$$s(\mathbf{k}) = \Delta k_x \Delta k_y$$

d. Justification for the method Why this procedure works? Here’s my understanding. I pay attention to two aspects, verifiability of both of which justify its validity. They are *equivalence to the original integral* and *gauge independency*.

Equivalence to the original integral Look at Eq.(2), the n th band Chern number is summation over the angle of the n th diagonal element of T_{loop} at all plaquettes. Then what the n th diagonal element of T_{loop} at each

plaquette exactly is? It is actually

$$\begin{aligned} T_{\text{loop}}^{(nm)}(x_i, y_i) &= (\mathcal{U}_{41}\mathcal{U}_{34}\mathcal{U}_{23}\mathcal{U}_{12})_{nn} = \mathcal{U}_{41}^{(nm)}\mathcal{U}_{34}^{(nm)}\mathcal{U}_{23}^{(nm)}\mathcal{U}_{12}^{(nm)} \\ &= \langle n(\mathbf{k}_1)|n(\mathbf{k}_4)\rangle\langle n(\mathbf{k}_4)|n(\mathbf{k}_3)\rangle\langle n(\mathbf{k}_3)|n(\mathbf{k}_2)\rangle\langle n(\mathbf{k}_2)|n(\mathbf{k}_1)\rangle \end{aligned}$$

But we know $\mathbf{k}_1, \mathbf{k}_2, \mathbf{k}_3, \mathbf{k}_4$ is four corners of a plaquette of the discretized parameter space, so that they are nearly next to each other and form a directional loop. Hence the a typical element is evaluated, up to first order, as

$$\begin{aligned} \langle n(\mathbf{k}_2)|n(\mathbf{k}_1)\rangle &= \langle n(x_{i+1}, y_j)|n(x_i, y_j)\rangle \\ &= (\langle n(x_i, y_j)| + \Delta k_x \langle \partial_x n(x_i, y_j)|) |n(x_i, y_j)\rangle \\ &= 1 + \Delta k_x \langle \partial_x n(x_i, y_j)|n(x_i, y_j)\rangle \\ &= 1 - \Delta k_x \langle n(x_i, y_j)|\partial_x n(x_i, y_j)\rangle \\ &= 1 + i \int_1^2 \mathcal{A}(x_i, y_j) d\mathbf{k}_x \end{aligned}$$

Similarly are other elements. Thus, to first order again, we obtain

$$T_{\text{loop}}^{(nm)}(x_i, y_i) = 1 + i \oint_{\square} \mathcal{A}(\mathbf{k}) \cdot d\mathbf{k} = e^{i\theta(\mathbf{k})}$$

and $\theta(\mathbf{k})$ is the $\mathbf{k} = (x_i, y_j)$ plaquette's contribution to whole Berry curvature integral. Adding all such terms is the Chern number (times 2π). This is guaranteed by Stokes' theorem.

Gauge independency A simple argument is that Chern number c_n is gauge invariant. So what we got is what we want to get, no concern about gauge smoothing.

But such an argument is somewhat tricky. If it just picks up one gauge at one point and another at another, arbitrarily, what happens at all? Is above derivation valid as well? Let we look at it explicitly. Suppose

$$|n(\mathbf{k})\rangle \rightarrow e^{i\chi(\mathbf{k})} |n(\mathbf{k})\rangle$$

then

$$\begin{aligned} T^{(n)}(\mathbf{k}) &= \langle n(1)|n(4)\rangle\langle n(4)|n(3)\rangle\langle n(3)|n(2)\rangle\langle n(2)|n(1)\rangle \\ &\quad \times e^{i[\chi(1)-\chi(2)+\chi(2)-\chi(3)+\chi(3)-\chi(4)+\chi(4)-\chi(1)]} \\ &= \langle n(1)|n(4)\rangle\langle n(4)|n(3)\rangle\langle n(3)|n(2)\rangle\langle n(2)|n(1)\rangle \end{aligned}$$

Being gauge invariant, this quantity. This is actually the fact that Berry curvature is a gauge independent quantity.

In conclusion, we trust this method gives valid numerical evaluation of the value of Chern number for a gapped band, and this method is of a merit that need not doing gauge smoothing for wave functions.

e. Precision accuracy How valid is this method? Here's some numerical results.

<pre>In[32]:= NumberForm[c1, 16] NumberForm[c2, 16] Out[32]//NumberForm= 0.9999999999999996 Out[33]//NumberForm= -1.0000000000000001</pre> <p style="text-align: center;">(a) case in Fig. 3</p>	<pre>In[61]:= NumberForm[c1, 16] NumberForm[c2, 16] Out[61]//NumberForm= -4.864810407253438 × 10⁻¹⁶ Out[62]//NumberForm= -1.260738261797028 × 10⁻¹⁷</pre> <p style="text-align: center;">(b) case in Fig. 5</p>
--	---

FIG. 2: Mathematica numerical results of Chern numbers for Rice-Mele model

We see that, the numerical accuracy can reach at a level $\ll 10^{-10}$ for the 1st Chern number.

II. CHERN NUMBER IN HIGHER DIMENSIONS

We could generalise the “Wilson loop” method to calculate non-Abelian Berry curvatures as well as Chern number in high dimensions. The case for non-Abelian Berry curvatures is merely a straightforward generalization of the non-Abelian case, and could be included in that for higher dimensional Chern number. This has also been discussed in Ref[1]. So we focus here on higher dimensional Chern number, specifically, the 2nd Chern number.

The 2nd Chern number is defined as[3, 4]

$$C_2 = \frac{1}{32\pi^2} \int d^4k \epsilon^{\mu\nu\rho\lambda} \text{Tr}[\mathcal{F}_{\mu\nu} \mathcal{F}_{\rho\lambda}] \quad (3)$$

where

$$\begin{aligned} \mathcal{F}_{\mu\nu} &= \partial_\mu \mathcal{A}_\nu - \partial_\nu \mathcal{A}_\mu + i[\mathcal{A}_\mu, \mathcal{A}_\nu] \\ \mathcal{A}_\mu^{\alpha\beta} &= (\mathcal{A}_\mu)^{\alpha\beta} = i\langle \alpha(k) | \partial_\mu \beta(k) \rangle \end{aligned} \quad (4)$$

Here superscript $\alpha\beta$ denotes band index, or in other words, matrix element of \mathcal{A}_μ . Notice that my convention here is not the same as that in Ref[3] and Ref[4] Chapter 13, but consistent with that in above section in this note.

a. antisymmetry reduction If we arrange four indices $ijkl$ in a way that 1234 is a “right” order such that

$$\epsilon^{ijkl} = \begin{cases} +1, & ijkl \text{ even with } 1234 \\ -1, & ijkl \text{ odd with } 1234 \end{cases}$$

then there are in total 24 non-zero ϵ^{ijkl} values, listed in the following (see Table I), together with the corresponding $\mathcal{F} \wedge \mathcal{F}$ term in the integral in Eqn.(3). It is clear that there are only 3 distinct $\mathcal{F} \wedge \mathcal{F}$ terms in the integral (or summation) in Eqn.(3), attributed to the antisymmetry of \mathcal{F} tensor. Hence we reduce Eqn.(3) in calculation to three distinct integral(summation) as

$$\begin{aligned} & \frac{1}{4\pi^2} \int dk_1 dk_2 \int dk_3 dk_4 \text{Tr}[\mathcal{F}_{12} \mathcal{F}_{34}] \\ & - \frac{1}{4\pi^2} \int dk_1 dk_3 \int dk_2 dk_4 \text{Tr}[\mathcal{F}_{13} \mathcal{F}_{24}] \\ & \frac{1}{4\pi^2} \int dk_1 dk_4 \int dk_2 dk_3 \text{Tr}[\mathcal{F}_{14} \mathcal{F}_{23}] \end{aligned}$$

and C_2 is the summation of these three.

TABLE I: non-zero value for antisymmetric tensor ϵ^{ijkl} and the corresponding $\mathcal{F} \wedge \mathcal{F}$ term in the integral

ϵ^{ijkl}	value	$Tr[\mathcal{F}_{\mu\nu}\mathcal{F}_{\rho\lambda}]$
ϵ^{1234}	1	$Tr[\mathcal{F}_{12}\mathcal{F}_{34}]$
ϵ^{2134}	-1	
ϵ^{1243}	-1	
ϵ^{2143}	1	
ϵ^{3412}	1	
ϵ^{4312}	-1	
ϵ^{3421}	-1	
ϵ^{4321}	1	
ϵ^{1324}	-1	$-Tr[\mathcal{F}_{13}\mathcal{F}_{24}]$
ϵ^{3124}	1	
ϵ^{1342}	1	
ϵ^{3142}	-1	
ϵ^{2413}	-1	
ϵ^{4213}	1	
ϵ^{2431}	1	
ϵ^{4231}	-1	
ϵ^{1423}	1	$Tr[\mathcal{F}_{14}\mathcal{F}_{23}]$
ϵ^{4123}	-1	
ϵ^{1432}	-1	
ϵ^{4132}	1	
ϵ^{2314}	1	
ϵ^{3214}	-1	
ϵ^{2341}	-1	
ϵ^{3241}	1	

b. Wilson loop construction We now generalise the procedure in Sec. I to non-Abelian case. The essential is still to discretize parameter space and consider every $\mathcal{F}_{\mu\nu}\Delta_\mu\Delta_\nu$, turning it into a Wilson loop in each discretized plaquette in higher dimensional parameter space. Notice that the form of \mathcal{F} tensor in Eqn.(4) producted with plaquette area should contain 2nd order terms in wavefunctions (of considering bands) so we extend our Wilson loop expansion to the 2nd order consistently. That is,

$$\begin{aligned}
|\alpha(k + \Delta_\mu)\rangle &= |\alpha(k)\rangle + |\partial_\mu\alpha(k)\rangle\Delta_\mu + \frac{1}{2}|\partial_\mu^2\alpha(k)\rangle\Delta_\mu^2 \\
\langle\alpha(k + \Delta_\mu)| &= \langle\alpha(k)| + \langle\partial_\mu\alpha(k)|\Delta_\mu + \frac{1}{2}\langle\partial_\mu^2\alpha(k)|\Delta_\mu^2
\end{aligned}$$

Hence the "link matrix" U_{12} in Sec.I procedure 4 is, taken 2 band model as an example, actually

$$\begin{aligned}
\begin{pmatrix} \langle\alpha(k + \Delta_\mu)|\alpha(k)\rangle & \langle\alpha(k + \Delta_\mu)|\beta(k)\rangle \\ \langle\beta(k + \Delta_\mu)|\alpha(k)\rangle & \langle\beta(k + \Delta_\mu)|\beta(k)\rangle \end{pmatrix} &= \begin{pmatrix} 1 & 0 \\ 0 & 1 \end{pmatrix} + i\Delta_\mu \begin{pmatrix} i\langle\alpha(k)|\partial_\mu\alpha(k)\rangle & i\langle\alpha(k)|\partial_\mu\beta(k)\rangle \\ i\langle\beta(k)|\partial_\mu\alpha(k)\rangle & i\langle\beta(k)|\partial_\mu\beta(k)\rangle \end{pmatrix} \\
&\quad - \frac{1}{2}\Delta_\mu^2 \begin{pmatrix} \langle\partial_\mu\alpha|\partial_\mu\alpha\rangle & \langle\partial_\mu\alpha|\partial_\mu\beta\rangle \\ \langle\partial_\mu\beta|\partial_\mu\alpha\rangle & \langle\partial_\mu\beta|\partial_\mu\beta\rangle \end{pmatrix} \\
&= \mathbb{1} + i\mathcal{A}_\mu(k)\Delta_\mu - \frac{1}{2}\Delta_\mu^2''\partial_\mu\partial_\mu''
\end{aligned}$$

Then the Wilson loop emerges via matrices product along the loop encircling a plaquette in parameter subspace:

$$\begin{aligned}
U_{41}U_{34}U_{23}U_{12} &= (1 - i\mathcal{A}_\nu(k)\Delta_\nu - \frac{1}{2}''\partial_\nu\partial_\nu'')(1 - i\mathcal{A}_\mu(k + \Delta_\nu)\Delta_\mu - \frac{1}{2}''\partial_\mu\partial_\mu'') \\
&\quad \times (1 + i\mathcal{A}_\nu(k + \Delta_\mu)\Delta_\nu - \frac{1}{2}''\partial_\nu\partial_\nu'')(1 + i\mathcal{A}_\mu(k)\Delta_\mu - \frac{1}{2}''\partial_\mu\partial_\mu'') \\
&= (1 - i\mathcal{A}_\nu(k)\Delta_\nu + \mathcal{O}(\Delta^2))(1 - i\mathcal{A}_\mu(k + \Delta_\nu)\Delta_\mu + \mathcal{O}(\Delta^2)) \\
&\quad \times (1 + i\mathcal{A}_\nu(k + \Delta_\mu)\Delta_\nu + \mathcal{O}(\Delta^2))(1 + i\mathcal{A}_\mu(k)\Delta_\mu + \mathcal{O}(\Delta^2)) \\
&= 1 + i \oint_{\square} \mathcal{A}(\mathbf{k}) \cdot d\mathbf{k} + \mathcal{O}(\Delta^2) \\
&= \mathcal{P} e^{i \oint_{\square} \mathcal{A}(\mathbf{k}) \cdot d\mathbf{k}} \quad (\text{up to 1st order in } \Delta, \text{ that is the circumference of discretized plaquette.})
\end{aligned}$$

Here \mathcal{P} denotes path-ordered integral.

However, for non-Abelian case, especially in doing with higher dimensional Chern number, \mathcal{F} tensor contains commutator of \mathcal{A} explicitly, manifest itself up to at least second order in integral or discretized version of summation. Thus our construction above is not complete in the sense that it is accurate up to the first order. After some operation[8], the error could be partly reduced to give a approximate value of C_2 , with the fidelity that total error limited to 2%. This is in the case of discretized to $50 \times 50 \times 50 \times 50$.

c. tests and applications To test my program, we tried examples in Ref[3, 4]. $h(\mathbf{k}) = ((m + \sum_j \cos k_j), \sin k_1, \sin k_2, \sin k_3, \sin k_4)$. Resultes match. We then calculated our four-bands model, using this program, written as Pengfei's Hamiltonian

$$\begin{aligned}
\mathcal{H}(q_x, q_y, \theta_1, \theta_2) &= \Delta(\theta_1, \theta_2) \Gamma_0 \\
&\quad + [1 + \delta_x(\theta_1, \theta_2) + \cos q_x] \Gamma_1 \\
&\quad + \sin q_x \Gamma_2 \\
&\quad + [1 + \delta_y(\theta_1, \theta_2) + \cos q_y] \Gamma_3 \\
&\quad + \sin q_y \Gamma_4
\end{aligned}$$

It yields $C_2 = 1$ for the lowest two degenerate bands.

d. future improvement There are at least two ways so far to improve:

- increasing discretization. Costs capability of computer in n^4 . Quite straightforward.
- constructing to next order in the algorithm above. Needs some numerics skills.

Acknowledgments

I thank Ce Wang, Pengfei Zhang, and all other guys involved for helpful discussion. I thank particularly Ce Wang for the discussions tonight (2016-11-25) that illuminates me on the essentials for future improvement.

-
- [1] T. Fukui, Y. Hatsugai, and H. Suzuki, *Chern Numbers in Discretized Brillouin Zone: Efficient Method of Computing (Spin) Hall Conductances*, *J. Phys. Soc. Jpn.* **74**, 1674 (2005).
- [2] Di Xiao, Ming-Che Chang, and Qian Niu, *Berry phase effects on electronic properties*, *Rev. Mod. Phys.* **82**, 1959 (2010).
- [3] Xiao-Liang Qi, Taylor L. Hughes, and Shou-Cheng Zhang, *Topological field theory of time-reversal invariant insulators*, *Phys. Rev. B* **78**, 195424 (2008).
- [4] B. Andrei Bernevig with Taylor L. Hughes, *Topological Insulators and Topological Superconductors*, *Princeton University Press* (2013).
- [5] M. J. Rice and E. J. Mele, *Elementary Excitations of a Linearly Conjugated Diatomic Polymer*, *Phys. Rev. Lett.* **49**, 1455 (1982).
- [6] D. J. Thouless, *Quantization of particle transport*, *Phys. Rev. B* **27**, 6083 (1983).
- [7] Yoshiro Takahashi's group, *Topological Thouless pumping of ultracold fermions*, *Nat. Phys.* **12**, 296-300 (2016).
- [8] private discussion with Ce Wang

Appendix A: Time-dependent Rice-Mele model

Consider a time-dependent Rice-Mele model[2, 5, 7]. Hamiltonian writes

$$H(t) = \sum_j -(J + \delta(t))a_j^\dagger b_j - (J - \delta(t))a_{j+1}^\dagger b_j + h.c. + \Delta(t)(a_j^\dagger a_j - b_j^\dagger b_j)$$

Fourier transformed into (crystal) momentum space we obtain a Hamiltonian with parameters (q, t) as

$$\begin{aligned} \mathcal{H}(q, t) &= -2J \cos\left(\frac{qa}{2}\right)\sigma_x + 2\delta(t) \sin\left(\frac{qa}{2}\right)\sigma_y + \Delta(t)\sigma_z \\ &= \mathbf{h}(q, t) \cdot \boldsymbol{\sigma} \\ &= \begin{pmatrix} \Delta(t) & -2J \cos \frac{qa}{2} - i2\delta(t) \sin \frac{qa}{2} \\ -2J \cos \frac{qa}{2} + i2\delta(t) \sin \frac{qa}{2} & -\Delta(t) \end{pmatrix} \end{aligned}$$

The time dependence is holding in $\delta(t)$ and $\Delta(t)$. In general, we set up

$$\begin{aligned} \delta(t) &= \delta_0 + \delta \sin(\omega t) \\ \Delta(t) &= \Delta_0 + \Delta \cos(\omega t) \end{aligned}$$

The degeneracy point is $\delta(t) = 0, \Delta(t) = 0$ (if there is). Thus the evolution loop could enclose or not enclose the degeneracy point, relying on whether or not this condition could be reached. Specifically, if $-\delta < \delta_0 < \delta$ and $-\Delta < \Delta_0 < \Delta$, the evolution loop then encloses the degeneracy point, else not.

Treating (q, t) as two-dimensional parameter torus, we calculate the Chern number, for each of the two bands, defined by the mapping from this torus to a sphere through the direction of eigenvectors for each band [see Eq. (1)], using the algorithm stated in Sec. I.

a. *A typical evolution loop* corresponding to parameters in Ref.[7]

$$\begin{aligned} \delta_0 &= 0 & \delta/J &= 0.85 \\ \Delta_0 &= 0 & \Delta/J &= 8.5 \end{aligned}$$

Chern number for two bands are calculated as $c_1 = 1$ (lower band), $c_2 = -1$ (upper band).

b. *Several other evolution loops* listed here

Note that the "FrameTicks" N is the number of discretization.

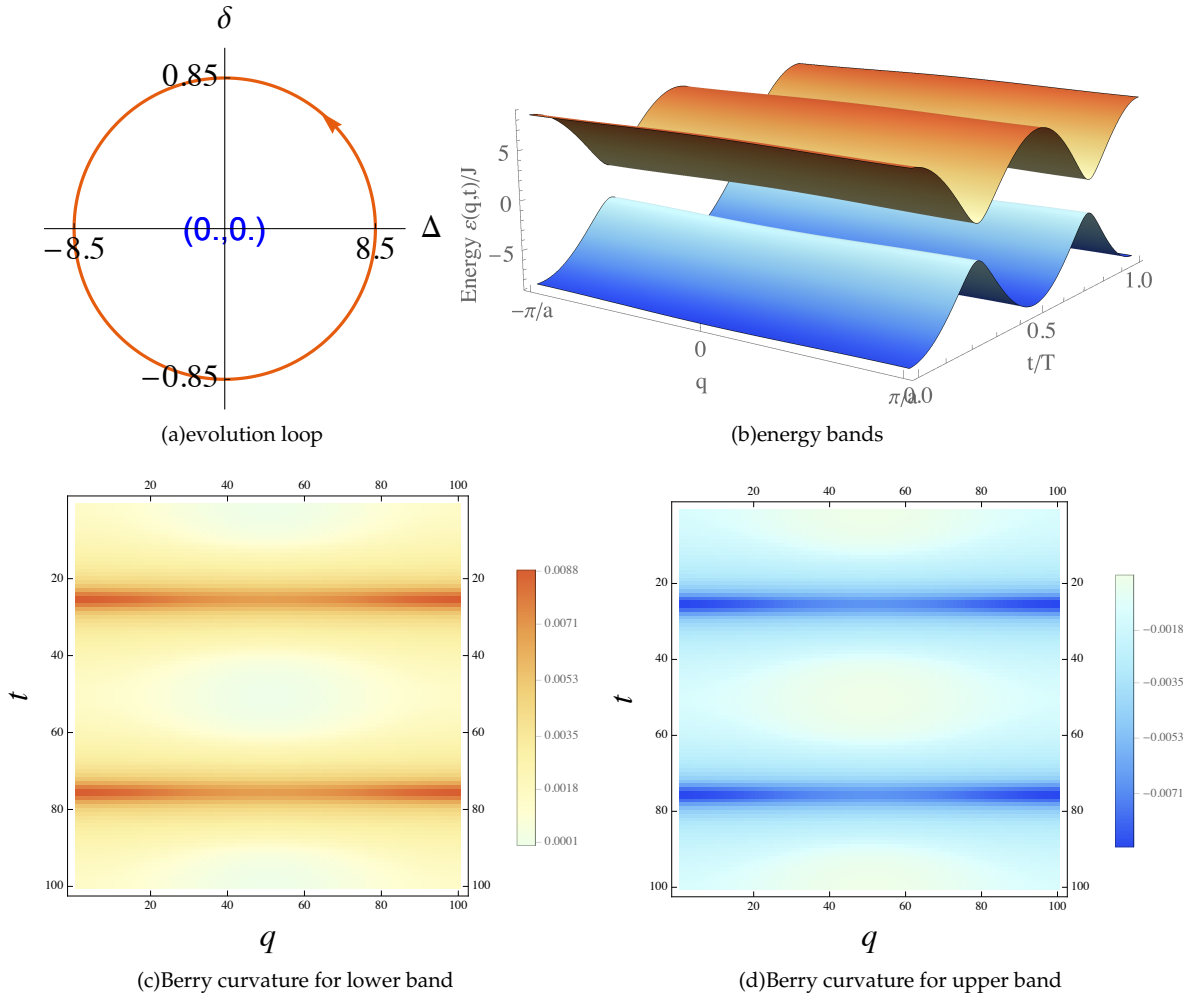
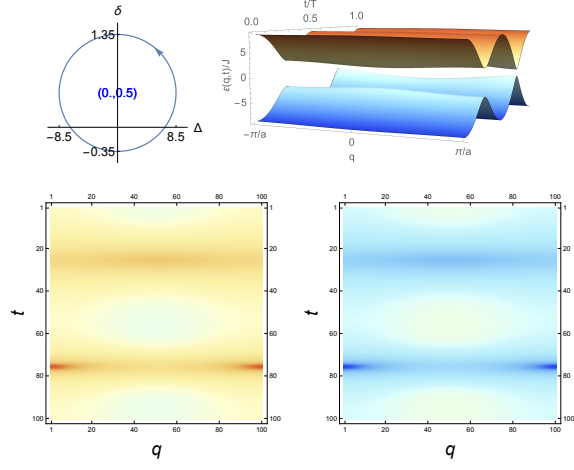
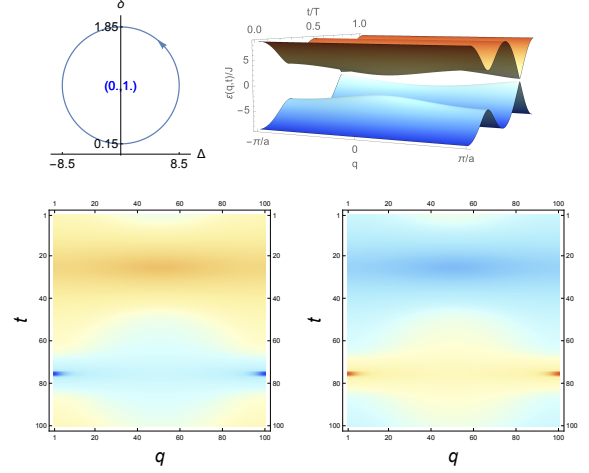
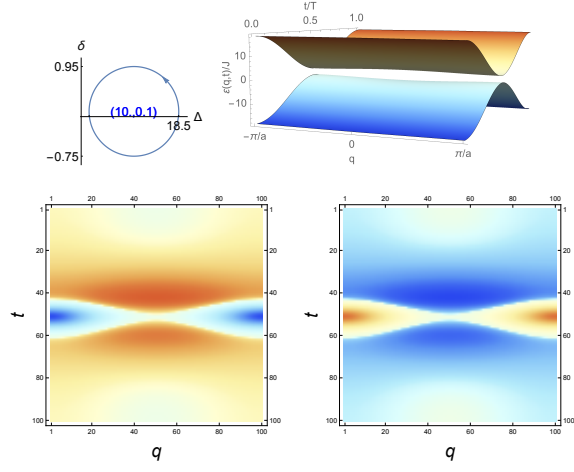
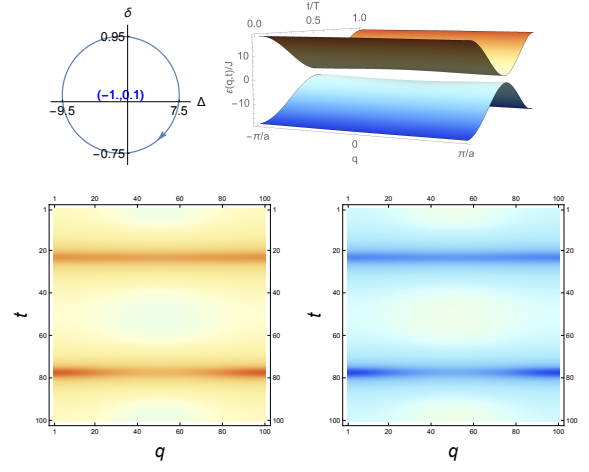
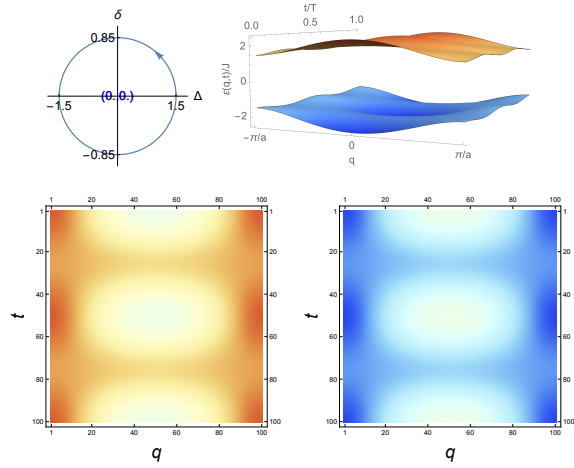
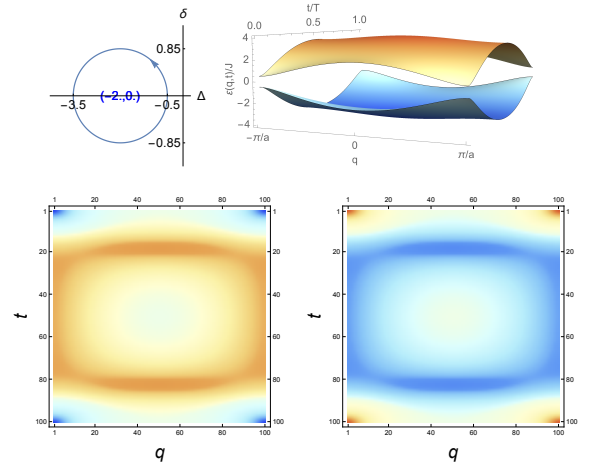


FIG. 3: Berry field for a typical evolution loop. Degeneracy point ($\delta = 0, \Delta = 0$) is enclosed by the loop.

FIG. 4: Degeneracy point is enclosed. $c_1 = 1, c_2 = -1$ FIG. 5: $(\delta = 0, \Delta = 0)$ is not enclosed. $c_1 = 0, c_2 = 0$ FIG. 6: $(0,0)$ not enclosed. $c_1 = 0, c_2 = 0$ FIG. 7: $(0,0)$ enclosed. Counterclock. $c_1 = -1, c_2 = 1$ FIG. 8: $(0,0)$ enclosed. With different parameter amplitude $\delta = 0.85, \Delta = 1.5$; $c_1 = 1, c_2 = -1$ FIG. 9: $(0,0)$ not enclosed. $\delta = 0.85, \Delta = 1.5$. Chern number $c_1 = 0, c_2 = 0$